Mechanism of the Trefonas Effect (Polyphotolysis) in Novolak−Diazonaphthoquinone Resists

Yu-Kai Han, Zhenglin Yan, and Arnost Reiser*

Institute of Imaging Sciences, Polytechnic University, Brooklyn, New York 11201

Received May 3, 1999; Revised Manuscript Received September 27, 1999

ABSTRACT: Polyphotolysis, namely the behavior of polyfunctional photoactive components (PACs), is an important aspect of dissolution inhibition resists. Polyfunctional PACs produce higher lithographic contrast and lead to higher line resolution. The effect is so important that trifunctional diazonaphthoquinone PACs have become the industry standard, virtually eliminating the use of the corresponding monofunctional inhibitors. We believe that polyphotolysis depends on an interaction between phenolic strings emanating from the acceptor groups of PACs located on the same backbone molecule. In the coating solution the strings of the PACs meet and connect with each other, and these connections survive into the solid resist film. After partial exposure some of the strings are severed from their anchors and would lose their inhibiting power, were it not for an unexpected effect that allows the severed strings to be reconnected to still polarized, "living" strings. In this process of reconnection the living strings increase in length, and the final result of exposure is the replacement of two shorter polarized strings by a single longer one. Inhibition depends on the overall number of phenolic units taking part in polarized strings. If there is only a small change in the overall length of the phenolic strings in the system, there will be only a small change in dissolution rate. That is precisely what Trefonas and Daniels observed.

Introduction

In the mid-1980s, Peter Trefonas and B. K. Daniels noticed that polyfunctional photoactive components (PACs) produced much higher lithographic contrast in Novolak resists than the corresponding monofunctional PACs. They called this phenomenon "polyphotolysis" and, in a remarkable paper,[2] examined it in detail: they monitored the dissolution rate and the bleaching of the diazonaphthoquinone (DNQ) moieties during irradiation of films containing a trifunctional DNQ PAC, and using a well-known simulation program,[3] they determined from these data that the photolysis of the first DNQ of the trifunctional PAC made almost no contribution to an increase in dissolution rate, photolysis of the second DNQ made a small contribution, and only when the third DNQ was converted to indenecarboxylic acid did the dissolution rate increase dramatically. This behavior accounts for the desirable nonlinear imaging characteristics of the system.

The Trefonas effect is illustrated in Figure 1 where we compare the exposure curves of two films, both made from the same Novolak resin and both containing the same overall number of identical DNQ-sulfate units. In one material the DNQ-sulfate units are distributed at random in the resin film, in the other, containing a trifunctional PAC, they are grouped together in threesomes. The final dissolution rate of the films is almost the same in both materials, but in the initial stages of exposure their behavior differs. In the films containing the trifunctional PAC the large increase in disslution rate is delayed. That means that the rate increase which produces most of the image must occur in a shorter exposure interval, hence the higher image contrast of the material. The Shipley group[4] assigned the phenomenon of polyphotolysis to a proximity effect[4] (see also the work of Uenishi et al.[5]). The presence of phenolic strings in the resist films opens now a way to a molecular interpretation of polyphotolysis; we believe that the effect is caused by the interaction of the phenolic strings emanating from the DNQ units of the trifunctional systems.

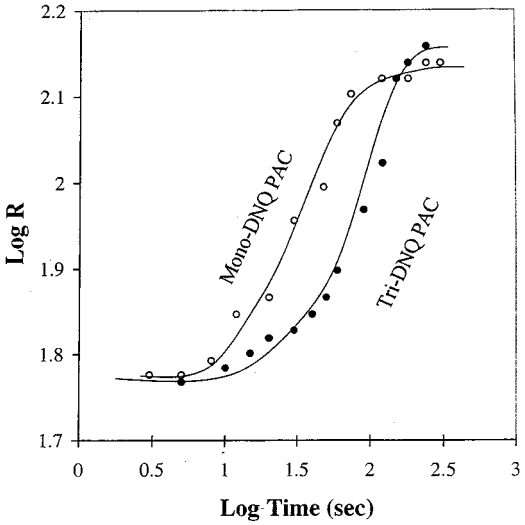

Figure 1. Exposure curves for two Novolak resists containing a monofunctional DNQ-5-sulfonic acid PAC and a similar trifunctional PAC based on 1,3,5-trihydroxybenzene. Both films contain the same overall diazonaphthoquinone concentration of 4.87×10^{-5} mol/kg of resin. The films were exposed to a UV lamp emitting 365 nm radiation, and their dissolution rate was measured by laser interferometry.

Phenolic Strings and Dissolution Inhibition

When a conventional PAC (a diazonaphthoquinone-sulfonic acid ester) is introduced into a phenolic solution, its hydrogen acceptors, the S=O units of the sulfonic acid moieties and the carbonyls of the DNQs, interact by hydrogen bonding with a nearby OH group and in so doing polarize it.

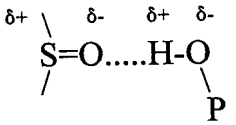

10.1021/ma990686j CCC: $18.00
Published on Web 11/20/1999

Table 1. String Length, *n*, and Mean pK_a of Free Phenols (pK_a(a)) and of Phenols Bound in Strings (pK_a(b)) (1.0 M Novolak Solutions in 95% Acetonitrile/5% Water)

	n	pK_a(a)	pK_a(b)
flavanone	14.5	7.35	7.59
flavone	15.0	7.37	7.83
α-naphthoflavone	16.8	7.37	8.00
sulfonic acid inhib	14.3	7.37	7.77

The oxygen atom of the polarized OH group is now a stronger hydrogen acceptor than the oxygen of a free phenol. It soon interacts with another OH group which in turn becomes polarized, attracts another OH group, etc. In this way strings of polarized phenols are formed.[6,7] We use the terms "strings" to refer to these sequences of hydrogen-bonded OH groups to distinguish them from the polymer chains that exist in these systems.

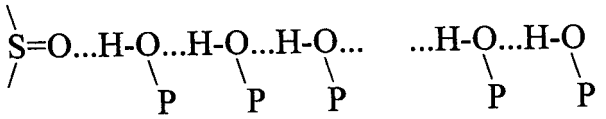

Phenolic strings are by no means a theoretical concept. Their real existence can be demonstrated by the effect of inhibitors on the viscosity of phenolic solutions and on the glass transition temperature of solid phenolic films.[8] Hydrogen bonding between the acceptor groups of the PAC and the OH groups of the phenols can also be documented by FTIR spectroscopy.[9]

Phenolic strings are characterized by two properties: their length and the mean acidity, or pK_a, of the OH groups contained in the strings.[10] The longer the strings and the higher the pK_a in the strings, the higher the inhibiting strength of the PAC. We shall express the inhibiting strength of a PAC by its inhibition factor, *f*, which is the negative slope of a plot of the logarithm of the dissolution rate[11] of films containing increasing concentrations, c_i, of the PAC

$$f = -\frac{\mathrm{d}\log R}{\mathrm{d}c_i} \tag{1}$$

It can be shown that the inhibition factor of a PAC can be related to the basic string properties by the expression[10]

$$f = n\frac{\log e}{c_{OH}}\left[1 - \frac{c_{H(b)}}{c_{H(a)}}\right] \tag{2}$$

where log *e* is 0.4343, c_{OH} is the overall concentration of OH groups in the system, and $c_{H(b)}$ and $c_{H(a)}$ are the proton concentrations in equilibrium with bound OH groups in the strings and with free OH groups in the bulk of the solution, respectively. These are readily derived from the corresponding pK_a values measured in solution. Table 1 gives values of string length and of the mean pK_a for a group of representative dissolution inhibitors introduced into a 1.0 M solution of Novolak in a medium of 95% acetonitrile and 5% water.[10]

Equation 2 has an interesting consequence. Since the ratio $c_{H(b)}/c_{H(a)}$ is a property of the acceptor groups of the PAC, for a given type of PAC, the inhibition factor *f* depends only on string length *n*. In polyfunctional PACs this, however, depends on the relative separation of the acceptor groups, as we shall see in the next section.

String Interactions

The string lengths in Table 1 were measured in dilute solutions where there is an unlimited supply of OH groups, and strings grow to their natural length. In concentrated solutions and with polyfunctional PACs the situation is different. In polyfunctional PACs strings originate near each other, and they start to interfere, in the sense that they prevent each other from reaching their natural length. That is reflected in the inhibition factors of polyfunctional PACs. For example, the *f*-number of a standard DNQ sulfonic acid ester in a representative Novolak resin is $f = 9.5$. The difunctional PACs shown below have much lower inhibition factors. (We are using here a symbolic notation where Q represents the DNQ-sulfonic acid motif).

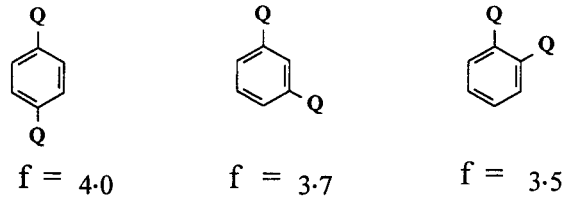

We interpret this as being the result of string interference. Strings originating at two acceptor (anchor) groups cannot merge, because they are polarized in the same direction, but they can interact with each other as electric dipoles.[12] When the polarized OH groups of the growing ends of two strings meet, they line up in a head-to-tail configuration and form a quadrupolar complex.

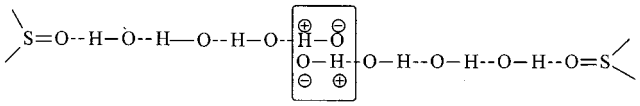

Within this structure the partial charges of the OH groups are compensated internally; they no longer project an external field strong enough to attract and hold another OH group. At the quadrupolar node the growth of both strings has come to an end.

String interactions are of particular interest in trifunctional PACs which play such an important role in practical microlithography. The question is, how do string interactions affect the behavior of trifunctional PAC before and after exposure?

Before we can deal with this question we need to recall what happens to a DNQ PAC during exposure.

What Happens on Exposure?

When the diazonaphthoquinone (DNQ) group of a standard PAC absorbs a quantum of radiation, it releases a molecule of nitrogen and, simultaneously, undergoes an intramolecular rearrangement. The sequence of steps associated with the exposure of DNQ unit is shown in Scheme 1. The so-called Wolff rearrangement[9] is highly exothermic and causes a heat pulse to be emitted from the location of the photolyzing DNQ. The resulting high-temperature spike breaks the hydrogen bond between the acceptor (S=O) and the OH group directly attached to it[14] and thereby severs the phenolic strings from its anchor. The severed string loses its polarization and becomes a mere sequence of ordinary phenols without any inhibiting properties. The severing of the phenolic string from the anchor group

Scheme 1

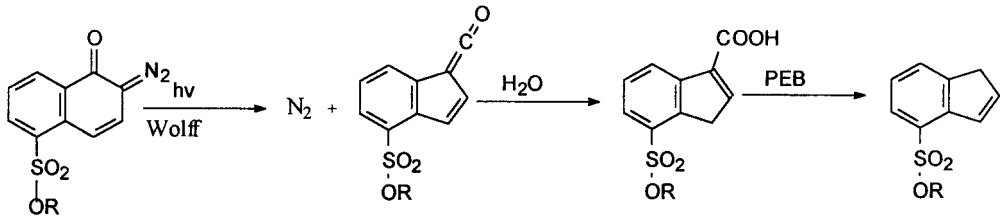

Scheme 2

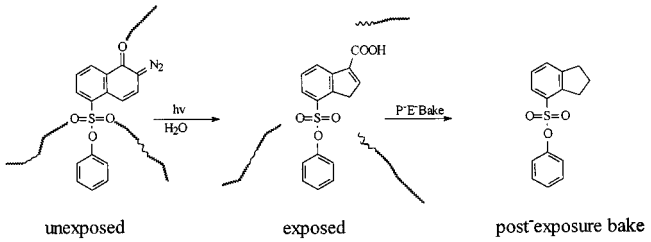

of the DNQ is the essential step of resist exposure. We have indicated this in Scheme 2.

At this point we note that the direct product of the Wolff rearrangement, a ketene, eventually adds one molecule of water and produces indenecarboxylic acid. Carboxylic acid is an electrolyte and as such acts as a dissolution promoter. However, a mild postexposure bake (70 °C for 1 h) removes the acid and leaves behind an indenesulfonic acid ester. Since the decarboxylation step is carried out in the solid matrix well below the glass transition temperature of the polymer, the undenesulfonic acid ester cannot form a new phenolic string in the rigid environment, and for that reason the indenesulfonate formed in these conditions has no effect on the dissolution rate. The return of the inhibited system to the dissolution rate of pure Novolak is illustrated in Figure 2 where we have plotted the logarithm of dissolution rate as a function of PAC content for a generic diazonaphthoquinone-5-sulfonic acid phenylester, before and after exposure and postbake.

Consider now the gradual exposure of a single molecule of a trifunctional DNQ PAC. Here the three DNQ groups react sequentially. The great merit of Trefonas' and Daniels' work is that they were able to distinguish the three phases of exposure and realize that the reaction of the first DNQ had almost no effect on the dissolution rate of the films, that the reaction of the second DNQ had a small effect (2%), and that only the reaction of the third and last DNQ produced a dramatic change in dissolution rate. Since dissolution rate is determined by the overall length of polarized phenolic strings, we may paraphrase Trefonas' and Daniels' findings by saying that in the first phase of exposure there is almost no change in the overall string length, that there is a small change in the second phase of exposure, and that only the reaction of the last DNQ brings about a large reduction in the length of the polarized strings. It is our contention that such a scenario may be realized if the severed strings can in some way be reconnected to the PAC molecule.

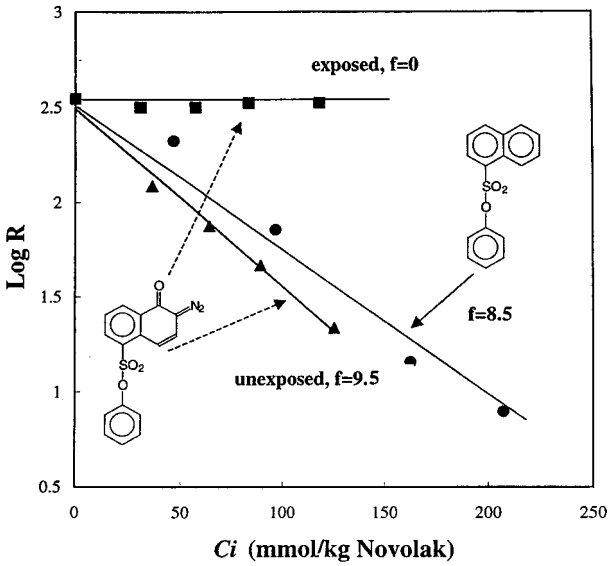

Figure 2. Meyerhofer plot of log *R* vs inhibitor concentration for a monofunctional DNQ-sulfonic acid PAC and for its nonphotoreactive naphthalenesulfonic acid analogue. The inhibition factors derived from these plots are indicated.

In the first exposure step of a trifunctional PAC the strings originating at the first DNQ-sulfonic acid unit are disconnected from their anchor groups, but they may be reconnected to the still living strings of the other two DNQ-sulfonic acid units to which they are linked at quadrupolar nodes. It requires only a slight movement of protons to make hydrogen bonding between the polarized strings and the phenols of the severed string possible. If that happens, the reconnected strings will be repolarized, their inhibiting power will be restored, and the inhibition factor of the system will not have changed. The driving force for reconnection is the high degree of polarization remaining in the living strings at the location of the quadrupolar nodes.

How can we test the hypothesis of string reconnection? We need to be able to calculate the behavior of a trifunctional PAC on the basis of string reconnection and then compare the prediction with the dissolution rates determined for the three stages of exposure. Trefonas and Daniels deduced the dissolution rates of monoexposed, biexposed, and triexposed PACs from experimental exposure curves similar to Figure 1, taking careful account of the statistics of double and triple exposures. We have found another way of separating the three stages of exposure. We prepared three mixed PACs on the basis of trihydroxybenzene. In PAC I only one OH group was substituted with a DNQ-sulfonic acid moiety while the two remaining positions were occupied by nonphotoreactive naphthalenesulfonic acid units. In PAC II two positions were occupied with DNQ-sulfonic acid groups; in PAC III all three positions were substituted with DNQ-sulfonic acid. The three PACs are shownin Scheme 3 in symbolic notation where Q and N stand for DNQ-sulfonic acid and naphthalenesulfonic acid, respectively. By exposing PAC I to completion, we simulate the first phase of the exposure of a trifunctional PAC; exposing PAC II to completion reproduces the second phase.

We turn now to the estimation of inhibition factors from string length. In the trifunctional PAC I the

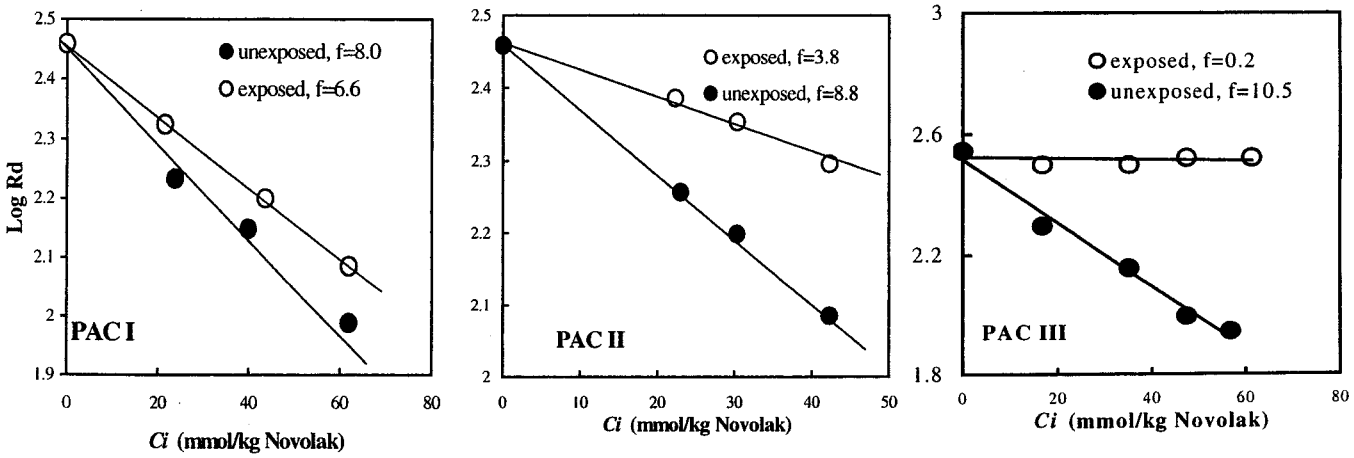

Figure 3. Meyerhofer plots for PACs I to III before and after exposure to completion.The inhibition factors are noted on the graphs. Films were coated on 2 in. silicon wafers and dissolved in 0.2 M KOH at 20 °C.

Scheme 3

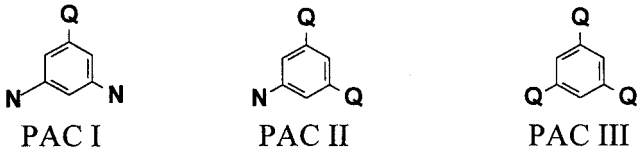

inhibition factor is determined by the length of six strings originating at the three sulfonic acid groups (we shall indicate their length by *a* and by the length of one string originating at the carbonyl oxygen of the DNQ (length *b*).

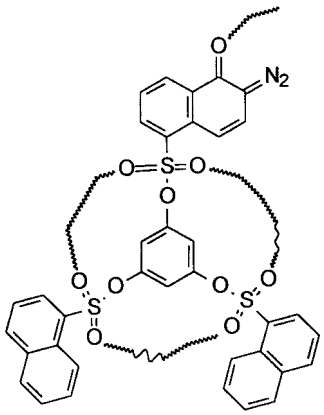

If string length is measured in units of inhibition factor, we may represent the inhibition factor of PAC I by the expression

$$f = 6a + 1b$$

We can estimate the value of *b* by comparing the inhibition factors ($f = 9.5$) of a standard monofunctional DNQ PAC such as the one shown in Figure 2 with the inhibition factor of the corresponding naphthalenesulfonic acid phenyl ester ($f = 8.5$) also indicated in the figure. It follows from this comparison that *b* has a value of unity.

$$b = 1.0 \text{ (units of inhibition factor)}$$

Since the strings originating at the quinone oxygen are presumably not involved in string interference, we shall assume that the value of *b* will be the same in the other mixed trifunctional PACs. From the measured inhibition factor of PAC I ($f = 8.2$) we obtain the value of *a*.

$$f = 6a + 1.0 = 8.2$$

$$a = 1.20$$

We are now ready to calculate the "expected" inhibition factors for the three mixed PACs *before exposure*.

PAC I: $f = 6a + 1b = 6 \times 1.20 + 1.0 = 8.2$

PAC II: $f = 6a + 2b = 9.2$ (experiment = 8.8)

PAC III: $f = 6a + 3b = 10.2$ (experiment = 10.5)

Calculating the inhibition factors of the three PACs *after exposure*, we assume that string reconnection occurs with an efficiency γ. The extreme cases of complete reconnection and no reconnection correspond to the values of $\gamma = 1$ and $\gamma = 0$.

We have experimentally determined the inhibition factors of the three mixed PACs before and after exposure from dissolution rate measurements on Novolak films containing increasing concentrations of the PACs (see Figure 3). Image contrast is the result of a change, Δf, in the inhibition factor on exposure.

$$-\Delta f = -[f(\text{exposed}) - f(\text{unexposed})]$$

Table 2. Inhibition Factor Changes in Mixed PACs

Δf	$\gamma = 0$	$\gamma = 1$	experim	$\gamma = 0.8$
PAC I	$2a + b = 3.4$	$b = 1.0$	1.40	1.48
PAC II	$4a + 2b = 6.8$	$4a = 4.4$	5.0	4.88
PAC III	$6a + 3b = 10.2$	$6a + 3b = 10.2$	10.3	10.2

For the three mixed PACs these data are collected in Table 2. The values of Δf for the two extreme cases of *no reconnection* and *complete reconnection* are noted in columns 2 and 3. The experimental values are in column 4. They are very close to the values in column 5 calculated for a reconnection efficiency of $\gamma = 0.8$.

In Figure 4 we have plotted the "expected" values of Δf for the three mixed PACs which de facto represent the three stages of exposure of a trifunctional PAC; the values of γ for the calculated data are indicated. We have included in the figure the experimental points derived from Figure 3. They come very near the "expected" trace for complete reconnection. While these data are strong support for the reality of string recon-

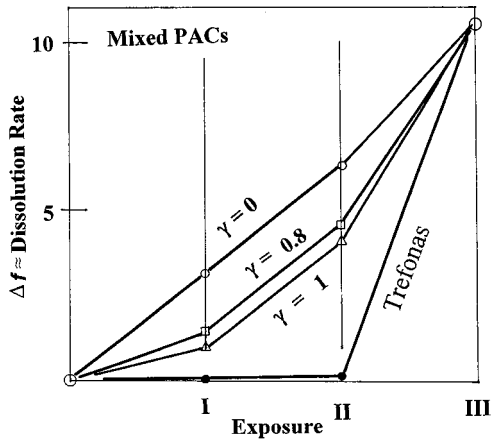

Figure 4. Schematic representation of the dissolution rate of PACs I to III, for the case of no reconnection of severed strings ($\gamma = 0$) and for the case of complete reconnection of severed strings ($\gamma = 1$). The experimentally found results indicate that reconnection occurs with an efficiency of 79% ($\gamma = 0.79$). The graph contains also the results of Trefonas and Daniels.[2]

nection, they still differ very much from Trefonas' and Daniels' results, which have also been entered into Figure 4. We believe that the discrepancy is caused by the large difference in the PAC concentration in the two sets of experiments. We have used concentrations of 2 g of PAC in 100 g of resin where the PAC molecules are isolated in the solid matrix. Trefonas' data were obtained under the more practical conditions of about 15 g of PAC in 100 g of resin. At these high concentrations strings of different molecules can interfere with each other. Strings originating at the quinone oxygen of the DNQ can now be reconnected to other strings, and so can strings that would not otherwise find reattachment point within their own molecules. In these conditions the loss of inhibiting power can be delayed until the last exposure step when no polarization center is available. That is what Trefonas' and Daniels' results indicate.

Spatial Limits of the Trefonas Effect

If the Trefonas effect is based on the interaction of strings originating at two or more inhibition centers, there must be spatial limits to the effect. This means that the reconnection efficiency will depend rather sensitively on the separation of the anchor groups at which the strings originate. When the separation between the anchor group increases, we expect the reconnection efficiency γ to decrease. If the distance between anchor groups becomes so large that the strings emanating from them do not interact with each other, the system will function like so many single PACs.

We have tested this proposition on the following four mixed PACs.

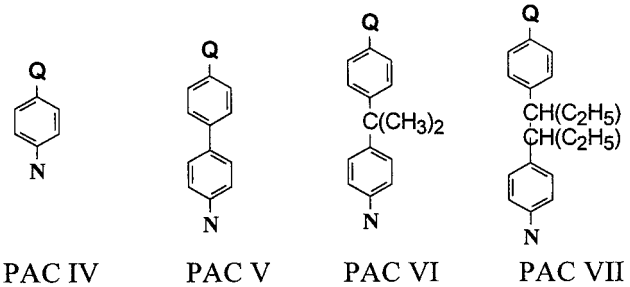

Their inhibition factors were measured before and after exposure and postbake. The inhibition factors of the four PACs in the unexposed and in the exposed and postbaked state are represented by the following expressions:

$$f(\text{unexposed}) = 4a + b$$

$$f(\text{exposed}) = 2a + 2a\gamma$$

$$\Delta f = 2a(1 - \gamma) + b$$

Assuming that b has the same value as in PACs I to III, namely $b = 1.0$, we have derived the string length values a from the inhibition factors of the mixed PACs before exposure and the reconnection efficiency, γ, from their inhibition factors after exposure. These data are listed in Table 3. As expected, the reconnection efficiency declines as the spatial separation of the anchor groups increases. The results have been plotted in Figure 5 for PACs IV, V, VI, and VII.

Table 3. Inhibition Factors String Length (a), Scavenging Efficiency (γ), and Separation (Δr) of Anchor Groups in Four Difunctional Mixed PACs

PAC	f(unexp)	f(exposed)	Δf	a	γ	Δr (Å)
IV	5.06	3.13	1.93	1.0	0.77	7.7
V	6.90	4.05	2.85	1.5	0.68	11.1
VI	8.16	4.33	3.83	1.8	0.59	12.8
VII	9.42	4.68	4.74	2.1	0.56	13.4

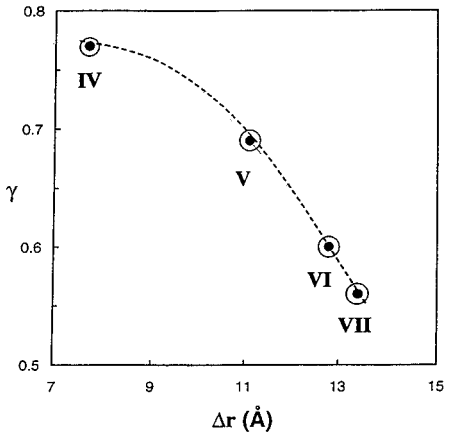

Figure 5. Effect of the spatial separation of the anchor group from which phenolic strings originate on the reconnection efficiency γ. The points in the graph refer to PACs IV to VII (see Table 3). Δr is the separation of the anchor groups, in angstrom units.

Experimental Part

Materials. Most of the starting materials were graciously donated by Honshu Chemical Industry Co. Ltd. (Japan) and by Mitsui Chemical America. Some others were purchased from Aldrich.

The mixed PACs were prepared starting from the corresponding dihydroxy- or trihydroxybenzene or the appropriate dihydroxy aromatics. In a first step the required number of OH groups was esterified with 1-naphthalene-5-sulfonyl chloride; in the second step the remaining OH groups were esterified with naphthalene-2,1-diazoquinone-5-sulfonyl chloride. A typical preparative procedure is described below.

Phloroglucinol or 4,4′,4″-methylidenetrisphenol (0.01 mol) was dissolved in 200 mL of dry THF. Triethylamine (0.01 or 0.02 mol) in 20 mL of dry THF was added slowly into the reaction flask over a period of 2 h. 1-Naphthalene-5-sulfonyl chloride (0.01 or 0.02 mol) in dry THF was also added. After stirring under nitrogen over 16 h, the solutions were added dropwise into a 0.05 N solution of HCl at 0° C. The precipitate formed was filtered off and washed with 0.05 N sodium

hydroxide. The product was finally crystallized from acetone/methanol (50/50) or from chloroform/methanol (50/50). The products of the first preparative step were fully characterized. These data are given below under PAC (a).

The product of this first step (0.01 mol) was dissolved in 200 mL of acetone containing 0.011, 0.022, or 0.033 mol of naphthalene-2,1-diazoquinone-5-sulfonyl chloride (DNQ-chloride). Triethylamine (0.012, 0.022, or 0.033 mol) dissolved in 50 mL of acetone was added slowly into the reaction flask over a period of 2 h. The pH of the solution was held between the values 7 and 8. After stirring under nitrogen for another 2 h, the solution was added dropwise into 0.01 N acetic acid at 0° C. The precipitate formed was filtered off, redissolved in acetone, and reprecipitated into an acetic acid solution. The precipitate was dried under vacuum at room temperature for 24 h.

The crude products of synthesis were chromatographed on silica gel columns to separate PACs I and II from each other. The chromatographed fractions were used for the final experiments.

Novolak resin was supplied through the good offices of Dr. Ralph Dammel by Clariant (formerly Hoechst). It was a resin based on 55% *m*-cresol and 45% *p*-cresol in the feedstock. The molecular weight M_w is 14 500 with a polydispersity of 6.

Materials Characterization. PAC I (a): mp = 191−192° C. ^{1}H NMR (200 MHz, $CDCl_3$): δ 6.6−7.0 (s, 3H), 7.38−7.48 (t,2H), 7.6−7.8 (m, 4H), 8.1−8.2 (q, 4H), 8.3−8.4 (d, 2H), 8.65−8.75 (d, 2H). Yield 71%.

PAC I: ^{1}H NMR (200 MHz, $CDCl_3$): δ 6.6−7.0 (s, 3H), 7.38−7.48 (m, 4H), 7.6−7.8 (m, 4H), 8.1−8.2 (m, 7H), 8.3−8.4 (d, 2H), 8.65−8.75 (m, 3H). Yield 80%.

PAC II (a): mp = 198−200 °C. ^{1}H NMR (200 MHz, acetone-d_6): δ 6.7−7.1 (s, 3H), 6.55−7.66 (t, 1H), 7.74−7.86 (m. 4H), 8.06−8.2 (m, 4H), 8.3−8.4 (d, 1H), 8.78−8.86 (m,4H). Yield 58%. PAC II: ^{1}H NMR (200 MHz, acetone-d_6): δ 6.7−7.1 (s, 3H), 6.55−7.66 (m, 4H), 7.74−7.86 (m, 4H), 8.06−8.2 (m, 4H), 8.3−8.4 (m, 3H), 8.78−8.86 (d, 2H). Yield 82%.

PAC III: ^{1}H NMR (200 MHz, acetone-d_6): δ 6.65−7.05 (s, 3H), 7.2−7.34 (d, 6H), 7.4−7.55 (d, 2H), 7.9−8.05 (d, 3H), 8.1−8.2 (dd, 4H). Yield 92%.

PAC IV (a): mp = 134−137 °C. ^{1}H NMR (200 MHz, $CDCl_3$): δ 6.5−6.7 (dd, 4H), 7.3−7.45 (t, 1H), 7.6−7.8 (m, 2H), 7.9−8.1 (m, 3H), 8.6−8.8 (dd, 1H). Yield 85%.

PAC IV: ^{1}H NMR (200 MHz, acetone-d_6): δ 6.5−6.7 (dd, 4H), 7.3−7.45 (t, 3H), 7.6−7.8 (m, 3H), 7.9−8.1 (m, 5H), 8.6−8.8 (dd, 1H). Yield 95%.

PAC V (a): mp = 155−156° C. ^{1}H NMR (200 MHz, acetone-d_6): δ 6.8−7.4 (qq, 8H), 7.55−7.65 (t, 1H), 7.7−7.9 (m, 3H), 8.3−8.4 (d, 1H), 8.55−8.6 (s, 1H), 8.75−8.85 (d, 1H). Yield 78%.

PAC V: ^{1}H NMR (200 MHz, acetone-d_6): δ 6.8−7.4 (qq, 8H), 7.55−7.65 (t, 3H), 7.7−7.9 (m, 4H), 8.1−8.2 (m, 3H), 8.3−8.4 (s, 1H), 8.75−8.85 (d, 1H). Yield 87%.

PAC VI (a): mp = 135−137° C. ^{1}H NMR (200 MHz, acetone-d_6): δ 2.2−2.25 (s, 6H), 6.7−7.0 (dd, 8H), 7.45−7.55 (t, 1H), 7.65−7.8 (m, 2H), 7.95−8.05 (d, 1H), 8.1−8.2 (d, 2H), 8.75−8.85 (d, 1H). Yield 72%.

PAC VI: ^{1}H NMR (200 MHz, acetone-d_6): δ 2.2−2.25 (s, 6H), 6.7−7.0 (dd, 8H), 7.45−7.55 (t, 3H),7.65−7.8 (m, 6H), 7.95−8.05 (d, 2H), 8.75−8.85 (d, 1H). Yield 87%.

PAC VII (a): mp = 105−108 °C. ^{1}H NMR (200 MHz, acetone-d_6): δ 0.4−0.5 (m, 6H), 1.2−1.3 (m, 4H), 2.4−2.6 (m, 2H), 6.7−7.1 (dd, 8H), 7.4−7.6 (t, 1H), 7.6−7.8 (m, 2H), 7.9−8.0 (d, 1H), 8.1−8.2 (d, 2H), 8.8−8.9 (d, 1H). Yield 65%.

PAC VII: ^{1}H NMR (200 MHz, acetone-d_6): δ 0.4−0.5 (m, 6H), 1.2−1.3 (m, 4H), 2.4−2.6 (m, 2H), 6.7−7.1 (dd, 8H), 7.4−7.6 (t, 3H), 7.65−7.8 (m, 4H), 7.95−8.05 (m, 2H), 8.1−8.2 (d, 2H), 8.8−8.9 (d, 1H). Yield 91%.

Dissolution Rate Measurements. Films were cast with a spin-coater from cyclohexanone solutions onto silicone wafers and dried for 1 h at 90 °C. The dissolution rate in 0.2 N KOH was measured at 20 °C using a single beam laser interferometer.[15] The inhibition factor was determined from the slope of Meyerhofer plots of the data.

Exposure and Postbake. The dry films were exposed for 2 min to a Hanovia mercury lamp, emitting mainly the G-line (437 nm). That exposure was twice that required for the complete transformation of the diazonaphthoquinone units into indenecarboxylic acid.

A set of fully exposed films was postbaked at 70 °C for increasing periods of time in a ventilated drying oven. The dissolution rate of the films was monitored after postbake. The dissolution rate of the exposed films had reverted to that of pure Novolak after a postbake of 35−40 min and did not change on longer treatment in the drying oven. Heating of the films for 2 h produced a densification of the material and somewhat lower dissolution rates.

Acknowledgment. We thank the Semiconductor Research Corporation and St. Jean PhotoChemicals (Canada) for financial support of this project, and we are grateful to Toshiko Takeno of Honshu Chemical Industry Co. (Tokyo) and to Greg Bushman of Mitsui Chemicals America for their generous help with some of the starting materials. We acknowledge with great pleasure helpful conversations with Peter Trefonas and Charles Szmanda (Shipley), with Trevor Clarke (St. Jean PhotoChemicals), with Grant Willson (University of Texas at Austin), and with Ralph Dammel (Clariant).

References and Notes

(1) Trevor Clarke, St. Jean Photochemicals, St. Jean-sur-Richelieu, Quebec: global shipping data on Novolak resists.
(2) Trefonas, P.; Daniels, B. K. *Proc. SPIE* **1987**, *771*, 194.
(3) Kim, D. J.; Oldham, W. G.; Neureuther, A. R. *IEEE Trans. Electron. Devices* **1984**, *ED-31*, 12.
(4) Szmanda, Ch. R.; Zampini, A.; Madoux, D. C.; McCants, C. L. *Proc. SPIE* **1989**, *1086*, 363.
(5) Uenishi, K.; Kawabe, Y.; Kokubo, T.; Slater, S.; Blakeney, A *Proc. SPIE* **1991**, *1466*, 102.
(6) Reiser, A.; Shih, H. Y.; Yeh, T. F.; Huang, J. P. *Angew. Chem., Int. Ed. Engl.* **1996**, *33*, 2428.
(7) Reiser, A. *J. Imaging Sci. Technol.* **1998**, *42*, 15.
(8) Shih, H. Y.; Reiser, A. *Macromolecules* **1995**, *28*, 5595.
(9) Shih, H. Y.; Reiser, A. *Proc. SPIE* **1995**, *2438*, 305.
(10) Yan, Zh.; Reiser, A. *Macromolecules* **1998**, *31*, 7723.
(11) Meyerhofer, D. *IEEE Trans. Electron. Dev.* **1980**, *ED-27*, 921.
(12) Berry, R. S.; Rice, S. A.; Ross, J. *Physical Chemistry*; Wiley: New York, 1980; p 408 ff.
(13) Han, Y. K.; Reiser, A. *Macromolecules* **1998**, *31*, 8789.
(14) Shih, H. Y.; Reiser, A. *Macromolecules* **1996**, *29*, 2082.

MA990686J